

Modeling of Fluorescent Molecular Hydrogen in IC405

Kevin France

Department of Physics and Astronomy, Johns Hopkins University, Baltimore, MD 21218

france@pha.jhu.edu

ABSTRACT

Rocket observations of the reflection nebula IC 405 are presented, including a high quality spectrum of the exciting star and nebular scattered light in the FUV bandpass. These data show a rise in the ratio of nebular surface brightness to stellar flux of roughly two orders of magnitude towards shorter wavelengths across the bandpass of the instrument. A model of fluorescing molecular hydrogen in the nebula is developed as a possible explanation. The model emission spectrum is produced using values derived from recent observations made with the Far Ultraviolet Spectroscopic Explorer. This model illustrates the presence of fluorescent molecular hydrogen in IC 405, but we determine that the emission is not the dominant factor in the short wavelength increase. Other explanations and future directions are discussed.

1. Introduction

One method of determining the physical properties of gas and dust in the interstellar medium (ISM) is to study these objects where they interact with stars. Reflection nebulae offer an opportunity to study dust absorption and scattering properties, excitations of the atomic and molecular gas species present, and how they alter the intrinsic stellar spectrum. One measurement that can shed considerable light on the processes occurring in the nebula is the ratio its surface brightness to the stellar flux (S/F_*). In principle, this requires two measurements, a spectrum of the exciting star(s) and a separate spectrum of the nebular region. One way of making these measurements simultaneously is the use of an imaging spectrograph. Observations with an imaging, or long-slit, spectrograph allow spectra to be measured at each location on the long-axis of the slit (cross-dispersion direction of the diffraction grating), obtaining data over a finite angular size on the sky. This technique lends itself to the study of reflection nebulae, where the central star typically has a small angular separation from the gas and dust with which it interacts.

Such an observation was recently made of the reflection nebula IC 405 by a rocket-borne, long-slit spectrograph in the far-ultraviolet spectral region (900 – 1400 Å). Upon analysis, the data revealed an increase in the ratio of nebular surface brightness to stellar flux of approximately two orders of magnitude to shorter wavelengths across the bandpass of the instrument. This result is in contrast with similar measurements of other well studied reflection nebulae, NGC 2023 and NGC 7023, which show a constant ratio in this spectral region (4; 9). One possible explanation of this blue rise is a population of molecular hydrogen that is absorbing ultraviolet continuum radiation from the exciting star and producing fluorescent emission in extended regions of the nebula. The purpose of this paper is to model such a population and compare

the output to observations of the nebula in order to better understand the physical processes occurring there. Section 2 discusses IC 405 and the rocket observations that were made. Section 3 outlines the data analysis procedure and discusses the results of the observations. Our modeling process consists of producing a population of molecular hydrogen in the ground electronic state and exposing it to the ultraviolet radiation field from the exciting star. Using known molecular rate coefficients, the molecules will absorb these ultraviolet photons and then cascade back to the ground electronic state, and it is a spectrum of this reemission that is the model output. Details of the modeling process are discussed in section 4, while section 5 discusses the results and their implications for the physical conditions within the nebula. Additionally in section 5, a brief description is given of this model’s possible application to recent observations of the aurorae of the giant planets made with the Far Ultraviolet Spectroscopic Explorer (FUSE). We conclude with an appendix discussing additional evidence supporting our result: a new scattered light calibration technique and data from other space-borne observatories.

2. Sounding Rocket Observations of IC405

IC 405 is a reflection nebula in Auriga, traditionally known as *The Flaming Star Nebula*. It is illuminated by a central star, AE Aur (HD 34078), which is a runaway from the Orion Nebula. AE Aur is thought to have been ejected from Orion roughly 2.5 million years ago in a binary-binary interaction that led to the creation of the well studied τ Ori binary system (2). Consequently, AE Aur is moving with a large proper motion through the nebula (≈ 17 AU/yr), and has been traditionally observed to study spectral time variations. AE Aur is thought to be cospatial with the nebula at a distance of about 450 pc. It is bright in both the visible ($V = 6.0$) and the ultraviolet (HD 34078 – O9.5 Ve), although it is rather extincted ($E(B - V) = 0.53$).

IC 405 was observed by a rocket-borne, far-ultraviolet imaging spectrograph. A telescope focuses the target at the entrance aperture of the instrument, an evacuated Rowland Circle spectrograph, using a microchannel plate stack detector with a KBr photocathode, readout by a double delay-line anode. The spectrograph is kept at a vacuum of $\approx 10^{-8}$ torr, and isolated from the spectrograph section by a gatevalve that opens at the appropriate time in flight. The spectrograph and telescope sections share a common vacuum ($P < \text{few} \times 10^{-5}$ torr). A mirrored slitjaw lies at the telescope focus and a long slit ($12'' \times 200''$ projected on the sky) defines the entrance aperture to the spectrograph. The spectrograph achieves a pointing limited spectral resolution of ≈ 3 Å. The telescope section of the instrument consists of the Faint Object Telescope (FOT) and an Attitude Control System (ACS) startracker mounted aft of the telescope on a ‘spider’ that is fastened to an invar heat shield. The FOT is a 40 cm diameter Dall-Kirkham, with a focal ratio of ≈ 16 and SiC coated optics. The aft end of the telescope section is sealed by a vacuum door.

This experiment was launched aboard a Mark 70 Terrier-Black Brant IX sounding rocket (NASA flight number 36.198 UG) from White Sands Missile Range, New Mexico ($106^{\circ}3$ West, $32^{\circ}4$ North), on 09 February 2001 at 21:00 MST. The target is obtained by referencing the startracker to two bright guide stars (Sirius and Capella), then reorienting to the target. The obtained field is within a few arcminutes of the nominal target, and this field is relayed to the ground in real-time through a Xybion TV camera imaging the slit jaw ($20'$ field-of-view). Fine adjustments are performed with real-time ACS command uplinks to argon jets.

Data was obtained of IC 405 from our arrival at the target field to experiment turn-off ($T +150 - T +490$ seconds). The command uplinks were used to place HD 34078 into the slit, the total stellar integration time was roughly 106 seconds. During the flight, the pointing was adjusted to two previously defined offsets to sample other parts of the nebula. Figure 1 illustrates the long-slit spectrum of the star and nebula measured during the flight.

3. Data Analysis

Flight data were analyzed using IDL code customized to read the data as supplied by the telemetry system. A background subtraction can be made by measuring the flux on the detector after instrument turn-on, but prior to target acquisition. The primary source of background flux is geocoronal airglow from atomic hydrogen and oxygen. The data are also combined with absolute measurements of telescope mirror reflectivities and spectrograph quantum efficiencies, measured both before and after flight in the calibration facilities located at Johns Hopkins University. Well characterized detector effects are also removed. Instrumental scattered light profiles can be measured and are discussed in the Appendix.

The stellar spectrum can be measured by correcting for pointing changes and extracting the data from the detector region where the star was present. Figure 2 shows the spectrum of the HD 34078 obtained during the flight. The spectrum is of high quality ($S/N \approx 10-15$ at $R = 300$), and is consistent with previous FUV measurements. After the star is removed, the spectra from different regions within the nebula can be separated by "time-tagging" the data from a playback of the Xybion camera that shows the flight time. Figure 3 shows the spectra of the nebula immediately surrounding the star and at the first offset pointing (along a bright filament, $425''$ to the northeast). Due to the lower flux away from the star and the short integration times inherent to a sounding rocket flight, the data were rebinned to improve the signal quality. The flux at the second offset position was not appreciably different than the background.

Integrating the nebular spectra over the area of the slit allows one to measure the brightness. Once the nebular brightness and stellar flux have been measured, their ratio (S/F_*) gives a commonly used diagnostic of the properties of the nebula (4). It is in this ratio that our observations reveal their most striking feature, the ratio of nebular surface brightness to stellar flux displays a rise of roughly two orders of magnitude to the blue from 1400 to 900 Å. The case for this 'blueness' is strong for the nebular regions near the central star, and despite the decreased S/N for the nebular offset pointing, a similar trend appears to be present. Figure 4 shows the S/F_* ratios. This result is in rather stark contrast to previous observations of reflection nebulae. An identical measurement has been made for NGC 2023, using the same instrument and experimental set-up (4) and a similar observation was made of NGC 7023, using a combination of data from Voyager 2 and the Hopkins Ultraviolet Telescope (HUT), aboard Astro-1 (9).

Both NGC 2023 and NGC 7023 display a flat nebular surface brightness to stellar flux ratio across the FUV bandpass. Burgh et al. have modeled the dust scattering in NGC 2023 and determine that the observed spectrum is due to a decreasing albedo balanced by an increasing phase function asymmetry parameter (improved absorption efficiency balanced by more strongly forward scattering grains). Murthy et al. explain the flat spectrum in NGC 7023 by having a decreasing albedo balanced by an increase in the flux of fluorescent molecular hydrogen (H_2) across the bandpass.

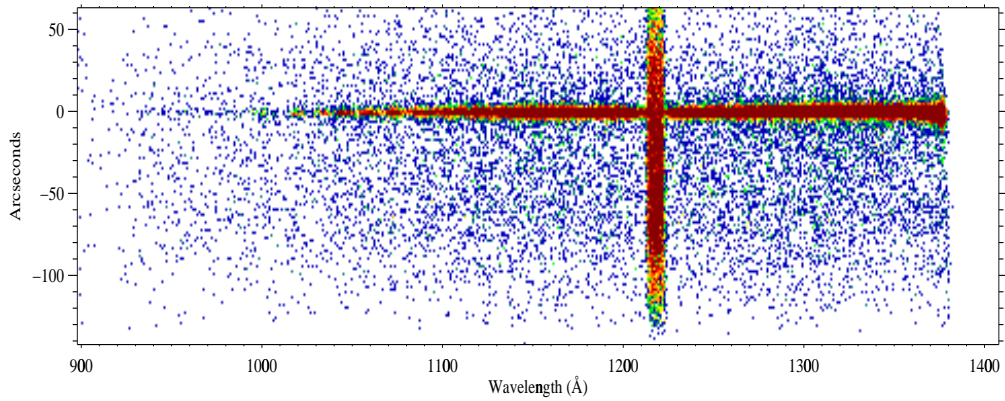


Fig. 1.— Raw flight data of HD 34078 and the surrounding nebula, after corrections for maneuvering, spectrograph alignment, and detector effects. In addition to the stellar and nebular flux, one notices the prominent hydrogen Ly- α airglow.

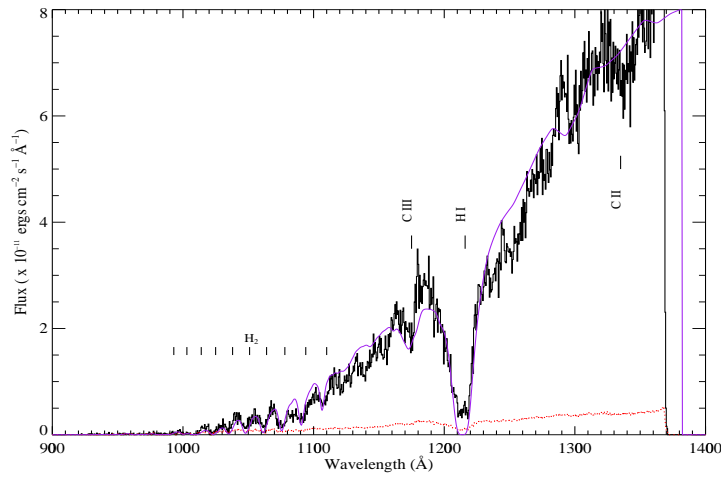


Fig. 2.— Flux calibrated spectrum of HD 34078, the central star in IC 405, overplotted with a Kurucz stellar model extinguished by a Fitzpatrick and Massa parameterization, and atomic and molecular hydrogen absorption (using a column density of 21.15, dominated by T = 80 K) along the line of sight – Error plotted as red broken line.

Several possibilities have been suggested to explain the blue rise that is exhibited in IC 405. Differential extinction within the nebula, such as a particular clump of dust along the line of sight, could explain the result. Determination of differential extinction is being pursued, and preliminary results are mentioned in section 5. Conventional dust scattering models suggest that the albedo of the nebula is significantly greater than unity, suggesting that an emission process of some sort is occurring. This emission could be produced either by the nebular dust or gas. Some sort of "extended blue emission" from dust is only speculative at this time, and emission from the nebular gas is the more traditional explanation. H_2 is an abundant molecule that has been observed to produce strong fluorescent emission in our bandpass, and the goal of this paper is to model a population of fluorescent molecular hydrogen to determine if it could be responsible for the observed S/F_\star ratio. FUV continuum longward of the Lyman limit, 912 Å, can be absorbed by hydrogen molecules and cause an electronic transition from the ground state to the Lyman and Werner bands. These excited electronic states then decay into discrete rovibrational states of the ground electronic state, emitting UV photons in the process (10). The combination of a strong source of FUV continuum (HD 34078), the large relative abundance of H_2 in the interstellar medium, and the fluorescent emission falling in the bandpass of our experiment have led us to investigate this as a possible explanation of our observations.

4. Modelling Procedure

Developing a model for a population of molecular hydrogen in IC 405 will allow us determine the possible contribution of fluorescence in the rise of the S/F_\star to shorter wavelengths. Such a model can be compared with the spectrum of the nebula obtained with our rocket experiment to determine the column densities of H_2 , or at least an upper limit. If the data is found to be consistent with model calculations, we can use the model to then predict the intensities of the individual rovibrational states that may be detected in emission during follow up observations at higher spectral resolution and sensitivity.

The modeling follows the method of Wolven et al. who were interested in modeling the fluorescent H_2 spectrum observed at the Shoemaker-Levy 9 impact site on Jupiter (12). That model used a single temperature, with a solar UV-field at 5 AU. The model that we develop for IC 405 will generalize the Jovian model to include two temperatures, corresponding to the rotational and vibrational temperatures, respectively. Additionally, we will revise the UV-field by allowing for different stellar types at different distances (for example, to illuminate our offset pointing, the UV-field would be produced by an O9.5 V type field, $T_{eff} = 32,000$ K, $\log(g) = 4$ at a distance of 0.88 pc).

A population of H_2 in its ground electronic state and in discrete rotational and vibrational states is created. This done by following the formalism of Herzberg to create a matrix of possible energy levels, characterized by their rotational and vibrational quantum numbers, j and v , respectively (6). The total energy of a state is given by the sum of the energies from each type of excitation, with E_e , the electronic energy equal to zero for the ground state. The total energy is then $E_{TOT} = E_{vib} + E_{rot}$. The energy levels can be expressed in terms of their wavenumbers (in units of cm^{-1}), for which vast tables of molecular constants

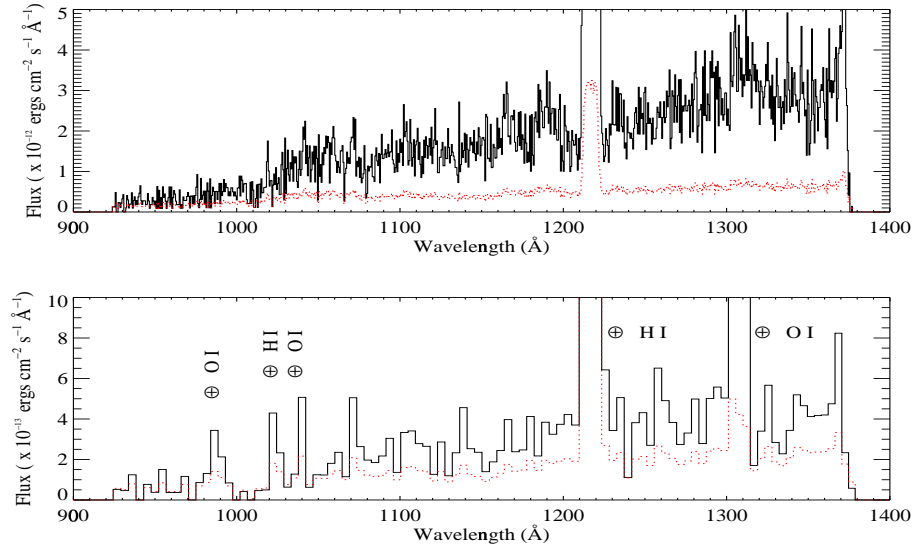


Fig. 3.— The top spectrum was obtained near HD 34078 during target acquisition and maneuvering. Below is the spectrum measured at a pointing offset, a position previously observed by the *Hopkins Ultraviolet Telescope*. Errors are plotted in red.

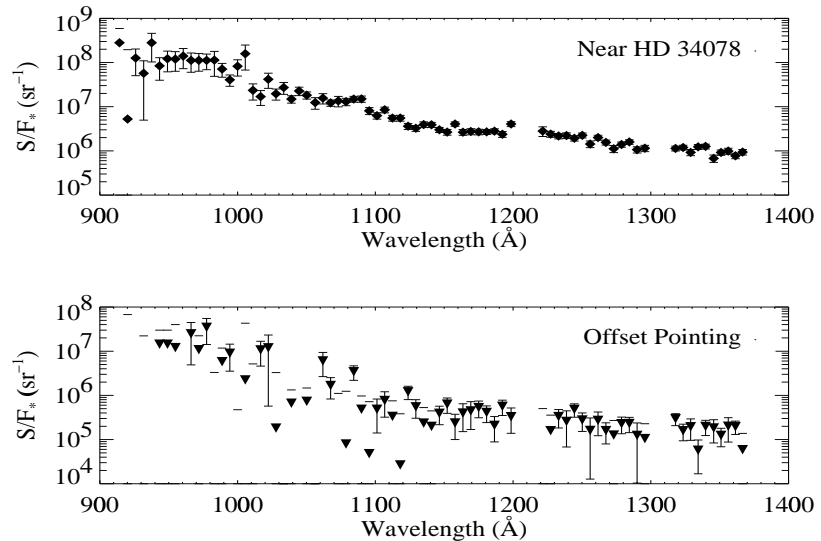


Fig. 4.— The ratio of nebular surface brightness to stellar flux rises by two orders of magnitude over the bandpass of the instrument, 1400 – 900 Å.

exist. The total energy as expressed in wavenumbers is then

$$\begin{aligned}\sigma &= \sigma_e + G + F \\ &\text{where} \\ G &= \omega_e(v + 1/2) - \omega_e \alpha_e (v + 1/2)^2 + \dots \\ F &= B_v j(j+1) - D_v j^2(j+1)^2 + \dots\end{aligned}\tag{1}$$

and σ_e is the wavenumber analog to the electronic energy ($= 0$). The ω_e terms above are molecular constants, but the B_v and D_v terms represent a coupling between the rotational and vibrational states. For example, one might imagine a high j -state "stretching" the molecule, producing anharmonicity in the vibrational potential, or the molecule's moment of inertia changing (and hence its rotational energy) as the molecule vibrates. To first order, these coupling terms can be expressed

$$\begin{aligned}B_v &= B_e - \alpha_e(v + 1/2) + \dots \\ D_v &= D_e - \beta_e(v + 1/2) + \dots\end{aligned}\tag{2}$$

where B_e , D_e , α_e , and β_e , are all molecular constants (7). It can be seen then that the energy can be decomposed into terms proportional to j , terms proportional to v , and a cross term that is approximately

$$\epsilon_{cross} = -3(v + 1/2)(j(j+1))\tag{3}$$

The wavenumber expressions of the energy are then converted back into units of energy (ergs), and an occupation probability of a given rovibrational state, $P(v, j)$, is found multiplying the Boltzmann factor by the degeneracy of a given state. The rotational and vibrational components of the energy are separated and assigned individual temperatures in the Boltzmann factor, which raises the question, what is the coupling temperature? In order to avoid this complication, a series of tests were run for single temperature models both with and without the cross term. We found that the cross term had a negligible effect on all vibrational states and rotational states of $j \leq 12$ for temperatures less than the collisional disassociation temperature (≈ 4000 K). This ground state population is then exposed to the UV-field described above, and excitation into the upper states are determined by theoretical rates at the Born limit, then re-emit using the calculated emission probabilities of Abgrall et al. (1). It is this emission spectrum that is the output of the model, with the rotational and vibrational temperatures and the total column density of molecular hydrogen, $N(H_2)$, as the inputs.

The model incorporates the option to manually input the column densities for each rovibrational state provided they can be determined by some other means. For example, recent FUSE observations of AE Aur have revealed a large column density along the line of sight, possibly associated with IC 405 (8). Le Petit et al. derive columns for the first 19 energy levels (starting at E(0,0)), and find a total column density of $N(H_2) = 6.4 \times 10^{20} \text{ cm}^{-2}$. Either the individual or total columns could be inputs into our model. Finally, this model could also be returned to the Jovian system to help explain recent FUSE observations of Jupiter and Saturn. At the time of this writing, several lines of H_2 present in the spectra of their aurorae are poorly fit by existing one temperature models.

5. Results

In this section, we present the preliminary results of our modeling efforts and a comparison of the model against flight data. In their analysis of the line of sight to HD 34078, Le Petite et al. report a column density

of $6.3 \times 10^{18} \text{ cm}^{-2}$ for the "warm" ($T > 80 \text{ K}$) molecular hydrogen and fit the higher lying absorption lines of H_2 as populations with temperatures of 400 and 1000 K, respectively (8). We adopt these values as nebular and use them ($N_{TOT} = 6.3 \times 10^{18} \text{ cm}^{-2}$, $T_{vib} = 1000$, and $T_{rot} = 400$) as our initial model inputs. The model output is an emission spectrum at a resolution of $R = 100,000$ at 1000 \AA . This spectrum is then convolved with a Gaussian profile that approximates the line-spread-function of the sounding rocket experiment ($\approx 3 \text{\AA}$ for the "near star" pointing). Figure 5 shows the nebular spectra with an overplot of the fluorescent emission model.

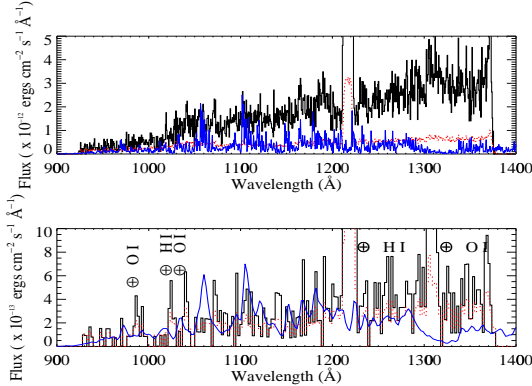


Fig. 5.— Nebular spectra with model emission spectra ($T_{rot} = 400$, $T_{vib} = 1000 \text{ K}$) overplotted in blue. Several lines are identified in the "near star" nebula, but there is little agreement with "off star" nebular position.

The comparison of the flight data with the model allows one to make the immediate conclusion that while there are several agreements between the model and the "near star" nebular region, the "off star" position is poorly fit by the model. This result is not entirely unexpected as the values input into the model were derived from observations of the nebula in the immediate vicinity of the star. Given the non-uniform appearance of IC 405, there is no reason to expect the values of temperature and column density to be the same in regions spatially separated by almost a parsec. Additionally, as HD 34078 is only passing through, it may not have had time to establish an equilibrium throughout the nebula. Near the star, we identify hydrogen emission lines near 1055, 1100, 1175, and 1230 \AA .

The analysis leading to the ratio of nebular surface brightness to stellar flux may be repeated, after subtracting the model from the nebular flight data, to produce a "hydrogen free" S/F_\star . We find that the S/F_\star ratio rises slightly less strongly, but that the contribution of the emission lines is negligible within the errors when compared with the order of magnitude scale effects we are exploring. Thus, despite the presence of fluorescent hydrogen emission in IC 405, we conclude that it is a higher order effect in determining the ratio S/F_\star . Figure 6 illustrates the analysis including the subtraction of the model, and little difference is discernible from Figure 4. The combination of the results presented here and initial work on exploring dust concentrations in the nebular region near the star leads us to believe that differential extinction is the explanation for the two order of magnitude rise in S/F_\star to shorter wavelengths. This differential extinction would most easily be explained as a clumpy dust distribution in the nebula, and in particular, that the central star lies behind a thin filament or small knot of dust. Preliminary efforts using an image reduction technique to expose the high frequency structure in the nebula and reduce saturation from the central star have indicated a dense and filamentary structure near the star. The technique employed is similar in spirit to the method

of unsharp masks (11) (this technique has also allowed us to identify Extended Red Emission in a nebular filament). A more rigorous determination of the extinction in the nebula may be made using hydrogen Balmer ratios and is the topic of future work.

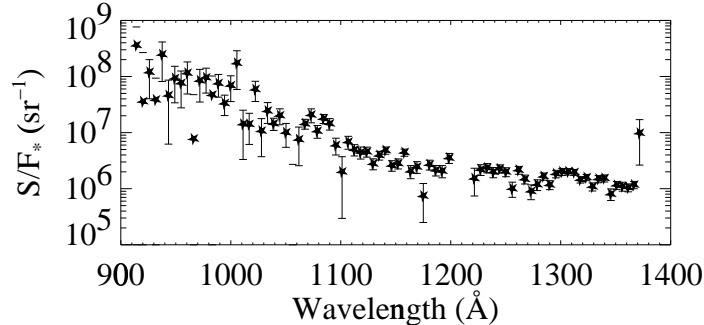


Fig. 6.— Repeating the nebular analysis with the fluorescent emission spectrum subtracted reduces shows little reduction in the S/F_{\star} rise to short wavelengths.

6. Closing

Spectra of the reflection nebula IC 405 have been obtained with a rocket-borne long-slit spectrograph in the 900 – 1400 Å region. The ratio of nebular surface brightness to stellar flux, S/F_{\star} , has been analyzed for two positions in the nebula and we have found a rise to shorter wavelengths of roughly two orders of magnitude across this bandpass. Various explanations have been proposed and this paper focused on the possibility that a population of fluorescent emission from molecular hydrogen was producing the blue nebular excess. A modeling procedure is outlined that assumes a population of molecular hydrogen in its ground state illuminated by a strong UV-field will be excited into upper electronic states and produce an emission spectrum as it cascades downward into discrete rovibrational states. The model uses a total column density derived from molecular hydrogen absorption along the line of sight to the central star, HD 34078 (8).

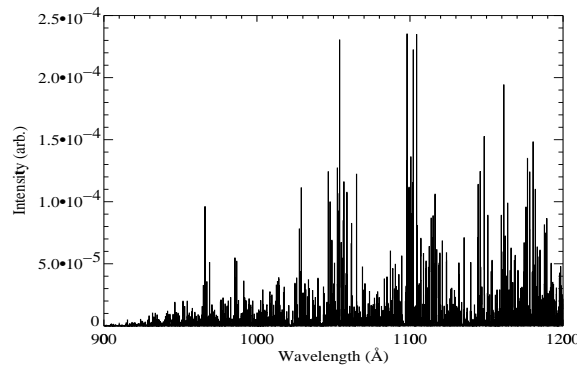


Fig. 7.— Model fluorescent emission spectrum as observed with high sensitivity and a spectral resolution of $\approx 20,000$.

We compared the model emission spectrum with the flight data by convolving it with the spectral profile of the rocket experiment. The model identified several features in the nebular spectrum obtained near the central star, but was a rather poor fit to the other nebular pointing. These identifications are interesting and warrant further observations at higher spectral resolution and sensitivity, see Figure 7, but are not sufficient in explaining the two order of magnitude rise in S/F_{\star} . Molecular hydrogen appears to be a higher order effect in the nebular brightness of IC405. The most plausible explanation at this time is differential extinction due to anisotropically distributed dust. Future work will allow this hypothesis to be more conclusively tested.

A. Scattered Light Calibration and Supporting Evidence

When these results were first presented at the 199th meeting of the American Astronomical Society, they were met with skepticism. Individuals familiar with the observational and theoretical properties of dust scattering in reflection nebulae suggested that our ‘blue’ S/F_* was a result of an instrumental effect, such as scattered light contamination. In addition to the fact that the result is a *ratio*, and therefore instrumental effects would tend to cancel themselves out, we present two additional arguments supporting the validity of our result, an end-to-end calibration of the instrumental scattered light profile and independent confirmation of our result using data from HUT and FUSE.

A.1. Vacuum Ultraviolet Collimator

FUV instrumentation requires testing and calibration in high vacuum environments to avoid contamination, operate microchannel plate detectors, and overcome the strong atmospheric attenuation of FUV light. Large vacuum calibration systems are expensive to build and maintain, and as a consequence, end-to-end testing of a vacuum ultraviolet optical system has traditionally been challenging. We have recently obtained a collimator used in calibrating FUSE, and fitted it with vacuum skins provided by Wallops Flight Facility (5). The collimator is a Cassegrain telescope, with a 381 mm primary diameter, a focal ratio of ≈ 12 , and SiC coated optics for improved FUV reflectance. The collimator vacuum skin tapers to 17.26 inches and couples to the aft end of the instrument section where it shares a vacuum with the Telescope and Spectrograph Sections. This allows for full end-to-end pre/postflight testing and calibration, including LSF and flat-field determination. A computer controlled motorized stage provides mounts for several light sources: a gas discharge pinhole lamp for point source simulation, an electron-impact lamp and a Bayard-Alpert ion gauge for filled aperture experiments. Precise knowledge of the LSF has enhanced the capabilities of the JHU sounding rocket experiment by allowing us to clearly distinguish between the profile of extended nebular flux and instrumental scattered light (5). Flat fielding gives us a better understanding of detector non-uniformities and permits a more complete calibration. Figure 8 shows a comparison between the scattered light profile determined using the vacuum collimator and the actual nebular extension that was observed during the flight.

A.2. Comparison with HUT and FUSE Archival Data

HUT, aboard Astro-2, observed IC 405 with a pointing very near to the nebular offset observation discussed above (unpublished). Combining this observation with the FUSE observation discussed above (3), allow us to reproduce the S/F_* determination with independent data sets. The nebular HUT spectrum can be integrated over area of the slit ($19'' \times 197''$) to measure the nebular surface brightness and the stellar FUSE spectrum can be convolved with an 8 Å Gaussian profile to roughly match the HUT filled-aperture resolution. These products can then be divided, and the resultant ratio spectrum shows the same \approx two order of magnitude rise towards the blue end of the spectrum, with an absolute offset due to the larger HUT aperture and the extraction of the stellar region from the rocket data. Figure 9 displays the HUT/FUSE analog to our measured S/F_* .

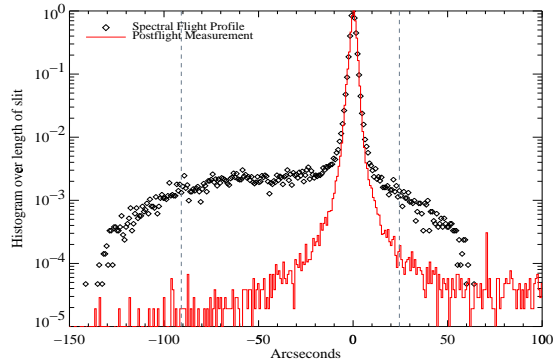


Fig. 8.— Spatial profile of the flight data in black (excluding Ly- α airglow). Postflight determination of the instrument line-spread-function (LSF) reproduces flight profile. The dashed lines represent the portion of the spectrograph slit unaffected by instrumental vignetting. One notices the extension of the nebula beyond the stellar peak.

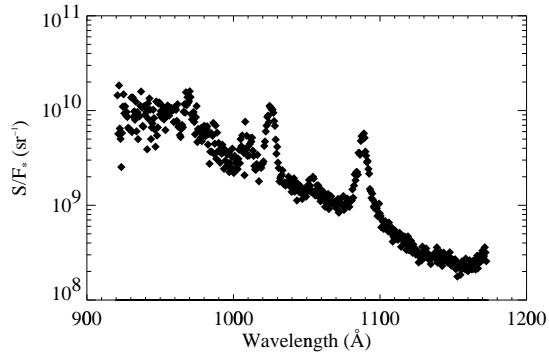


Fig. 9.— S/F_* determined using an IC 405 observation made by HUT and the spectrum of HD 34078 measured by FUSE, convolved to the lower spectral resolution of HUT. The features near 1025 and 1090 Å are due to strong Ly- β airglow and an error in the extraction of the FUSE data, respectively.

The author would like to thank Stephan McCandliss for his guidance in reducing the rocket data and preparing the model presented. The author would also like to thank Brian Wolven for constructing the original structure of the model and Eric Burgh for providing a framework for the analysis of the observational data. The author pays his respects to *DancePartyJuarez!*, which provided a countless measure of inspiration.

REFERENCES

- H. Abgrall, E. Roueff, F. Launay, J. Roncin, and J. Subtil. Table of werner band system of molecular hydrogen. *Astronomy and Astrophysics*, 101:323, 1993.
- W. G. Bagnuolo, R. L. Riddle, D. R. Gies, and D. J. Barry. τ orionis – evidence for a capture origin binary. *ApJ*, 554:362–367, 2001.
- P. Boisse, E. Rollinde, F. Le Petit, G. Pineau des Forets, E. Roueff, C. Gry, B-G. Andersson, and V. Le Brun. Small scale structure in diffuse molecular gas from repeated fuse and visible spectra of hd 34078. In *Proceeding of the IAP*, volume 17, 2002.
- E. B. Burgh, S. R. McCandliss, and P. D. Feldman. Rocket observations of far-ultraviolet dust scattering in ngc 2023. *ApJ*, ‘accepted’, 2002.
- E. B. Burgh, S. R. McCandliss, R. Pelton, K. France, and P. D. Feldman. Windowless vacuum ultraviolet collimator. In *Proceedings of the SPIE*, volume 4498, 2001.
- G. Herzberg. *Molecular Spectra and Molecular Structure*. D. Van Nostrand Company, 1950.
- G. Herzberg and H. Huber. *Constants of Diatomic Molecules*. D. Van Nostrand Company, 1960.
- F. Le Petite, P. Boisse, G. Pineau des Forets, E. Roueff, C. Gry, B-G. Andersson, and V. Le Brun. Fuse observations towards hd 34078 detection of highly excited h₂ and hd. *astro-ph*, 0110358:pre–print, 2001.
- J. Murthy, A. Dring, R. C. Henry, J. W. Kruk, W. P. Blair, R. A. Kimble, and S. T. Durrance. Hopkins ultraviolet telescope observations of far-ultraviolet scattering in ngc 7023 - the dust albedo. *ApJ*, 408:L97–L100, 1993.
- A. Sternberg. Ultraviolet fluorescent molecular hydrogen emission. *ApJ*, 347:863–874, 1989.
- A. N. Witt and D. F. Malin. The extended red emission filaments in ngc2023. *ApJ*, 347:L25–L27, 1989.
- B. C. Wolven, P. D. Feldman, D. F. Strobel, and M. A. McGrath. Ly-alpha-induced fluorescence of h₂ and co in hubble space telescope spectra of a comet shoemaker-levy 9 impact site on jupiter. *ApJ*, 475:835–842, 1997.